Benefits of Net Zero policies for future ozone pollution in China

Zhenze Liu[1,2], Oliver Wild[2], Ruth M. Doherty[3], Fiona M. O'Connor[4,5], and Steven T. Turnock[4,6]

[1]Jiangsu Key Laboratory of Atmospheric Environment Monitoring and Pollution Control, Collaborative Innovation Centre of Atmospheric Environment and Equipment Technology, School of Environmental Science and Engineering, Nanjing University of Information Science and Technology, Nanjing, China
[2]Lancaster Environment Centre, Lancaster University, Lancaster, UK
[3]School of GeoSciences, The University of Edinburgh, Edinburgh, UK
[4]Met Office Hadley Centre, Exeter, UK
[5]Department of Mathematics and Statistics, Global Systems Institute, University of Exeter, Exeter, UK
[6]University of Leeds Met Office Strategic Research Group, School of Earth and Environment, University of Leeds, Leeds, UK

Correspondence: Zhenze Liu (zhenze.liu@nuist.edu.cn)

Abstract. Net Zero emission policies principally target climate change, but may have a profound influence on surface ozone pollution. To investigate this, we use a chemistry-climate model to simulate surface ozone changes in China under a Net Zero pathway, and examine the different drivers that govern these changes. We find large monthly mean surface ozone decreases of up to 16 ppb in summer and small ozone decreases of 1 ppb in winter. Local emissions are shown to have the largest influence on future ozone changes, outweighing the effects of changes in emissions outside China, changes in global methane concentrations and a warmer climate. Impacts of local and external emissions show strong seasonality, with the largest contributions to surface ozone in summer, while changes in global methane concentrations have a more uniform effect throughout the year. We find that while a warmer climate has a minor impact on ozone change compared to the Net Zero scenario, it will alter the spatial patterns of ozone in China, leading to ozone increases in the south and ozone decreases in the north. We also apply a deep learning model to correct biases in our ozone simulations, and to provide a more robust assessment of ozone changes. We find that emission controls may lead to a surface ozone decrease of 5 ppb in summer. The number of days with high ozone episodes with daily mean ozone greater than 50 ppb will be reduced by 65 % on average. This is smaller than that simulated with the chemistry-climate model, reflecting overestimated ozone formation under present-day conditions. Nevertheless, this assessment clearly shows that the strict emission policies needed to reach Net Zero will have a major benefit in reducing surface ozone pollution and the occurrence of high ozone episodes, particularly in high-emission regions in China.

1 Introduction

Rapid changes in air pollution have occurred in China over the last few decades because of dramatic transformations in economic development and air pollutant emissions. Following substantial increases in emissions in the 1990s and 2000s, nationwide pollutant emission controls since 2013 have led to remarkable reductions in fine particular matter ($PM_{2.5}$), with national population-weighted annual mean concentrations decreasing from 62 to 42 g/m^3 during 2013-2017 (Zhang et al., 2019). However, surface ozone (O_3) pollution is becoming increasingly prevalent in China despite these emission controls, as recent

emission policies have primarily targeted fine particles (Wang et al., 2022a). Reductions in the emissions of nitrogen oxides (NO_x), a precursor of both O_3 and fine particles, may lead to increased O_3 concentrations due to non-linear O_3 chemistry (Liu et al., 2021) and to strengthened incoming solar radiation (Hollaway et al., 2019). In addition, anthropogenic emissions of

25   other O_3 precursors that contribute to O_3 formation e.g. volatile organic compounds (VOCs) and methane (CH_4) are less well regulated (Li et al., 2019). Observed summertime surface maximum 8h average (MDA8) O_3 concentrations in China showed a consistent annual increase of 1.9 ppb between 2013 and 2019 (Li et al., 2020), and this increase is greater in high-emission regions, reaching 3.3 ppb per year on the North China Plain. Given that O_3 production in these regions tends to be VOC-limited (Wang et al., 2022b), reducing emissions of NO_x and VOCs simultaneously has become crucial. There are also significant nat-

30   ural sources of O_3 precursors from vegetation and soils that may increase due to a warmer climate (Doherty et al., 2013; Fiore et al., 2015). Since surface O_3 is detrimental for human health, plant growth and crop yields (WHO, 2021), robust and effective emission controls on O_3 precursors are needed.

    The Intergovernmental Panel on Climate Change (IPCC) calls for cutting global greenhouse emissions to as close to zero to reduce the risks of climate change (IPCC, 2022). Many countries have recently adopted such Net Zero policies to reduce

35   net greenhouse gas emissions to zero by 2050, and China has also implemented emission policies that aim to achieve a carbon peak before 2030 and carbon neutrality by 2060 (Tay, 2022). These low-carbon policies alongside reductions in anthropogenic air pollutant emissions will have co-benefits for both global climate and air quality (UNEP, 2022). However, since surface O_3 changes are not directly proportional to emission changes, it is challenging to quantify the benefits for O_3 accurately. Future O_3 is also influenced by climate change through changes in atmospheric stagnation, natural emission sources, chemical reaction

40   rates, and deposition rates (Hong et al., 2019; Zanis et al., 2022; Brown et al., 2022). Regional surface O_3 changes also depend on emissions pathways in other parts of the world, which influence the long-range transport of O_3 and its precursors across continents (Wild et al., 2012; Doherty, 2015). The combination of these factors shapes the changes in future O_3 but imposes large uncertainties in O_3 projections (Turnock et al., 2020), which poses a challenge to assess the underlying impacts of Net Zero policies on future air quality.

45   While the general relationships between O_3, its precursor emissions and climate change are known well (Zeng et al., 2008; Hedegaard et al., 2013; Doherty et al., 2013; Griffiths et al., 2021), the relative importance of these drivers remains very uncertain. Challenges remain in the capability of chemistry-climate models to simulate O_3 changes accurately because processes occurring at small scales cannot be resolved adequately. Young et al. (2018) show that there are systematic biases in the simulation of present-day O_3 concentrations in current chemistry-climate models, and this raises questions over their skill in

50   representing long-term O_3 changes (Parrish et al., 2021). Averaging output from a number of different models is a common way to obtain more robust results, but does not eliminate the O_3 biases that are shown to be systematic (Revell et al., 2018). In addition, the models tend to use different parametrizations to represent different processes (Wild et al., 2020), and may misrepresent the importance of local emission controls or the risks caused by climate change. It is hence valuable to correct model simulations to produce more robust O_3 projections.

55   A practical way to address this is to apply deep learning models. Deep learning approaches have developed quickly in the last decade due to advances in computational speed that allow intensive training, and they have been applied widely in scientific

fields (LeCun et al., 2015). Deep learning models have been shown to be a universal approximator (Hornik et al., 1989) and can thus be applied to compensate for discrepancies between physical model simulations and observations. We have demonstrated a successful application of deep learning to correct the biases in surface O_3 simulations from a global chemistry-climate model (Liu et al., 2022b), and found that changes in surface O_3 in high-emission regions across the world may be overestimated with the process-based model. This bias correction approach allows us to provide a more robust and reliable assessment of future surface O_3 projections under the effect of different emission policies and facilitates an examination of their effectiveness.

The aim of this study is to produce reliable estimates of future O_3 changes associated with changing emissions and climate under a Net Zero pathway in China, and to determine how well strict emission controls can tackle the increasing frequency of high O_3 episodes. We introduce the chemistry-climate model used in Sect. 2 along with different emission and climate scenarios, and we describe the deep learning model that we have implemented to correct surface O_3 biases. ~~We then~~ In order to highlight the value of bias correction, we show the results of UKESM1 before showing the corrected results. We first investigate surface O_3 changes in China from the present day to the future under a Net Zero emission pathway simulated with UKESM1 in Sect. 3. The influences of emission changes outside China, changes in global CH_4 concentrations, and climate change are examined in Sect. 4. We demonstrate the capability of the deep learning model in simulating the biases in surface O_3, and apply this bias correction technique to estimate future O_3 changes and high O_3 episodes in Sect. 5. Conclusions are presented in Sect. 6.

2 Approach

2.1 Description and application of the chemistry-climate model

We use version 1 of the United Kingdom Earth System Model, UKESM1 (Sellar et al., 2019) to simulate surface O_3 mixing ratios in the present-day (2013?017) and the future (2060-2070) under different scenarios. UKESM1 consists of a physical climate model, the Hadley Centre Global Environment Model version 3 (HadGEM-GC3.1), configured with the Global Atmosphere 7.1 and Global Land 7.0 (GA7.1/GL7.0) components (Walters et al., 2019), to which other Earth system processes are coupled (Sellar et al., 2019). A state-of-the-art module for modelling atmospheric composition in the troposphere and the stratosphere, the United Kingdom Chemistry and Aerosol model (UKCA; Morgenstern et al., 2009; O'Connor et al., 2014) is included. A gas-phase chemistry scheme, StratTrop (Archibald et al., 2020b) and an aerosol scheme, GLOMAP-mode (Mulcahy et al., 2020) are used in UKCA. An extended chemistry scheme based on StratTrop that incorporates more reactive VOC species including alkenes, alkanes, and aromatics is used in this study to permit a more realistic representation of the chemical environment in China (Liu et al., 2021). The model resolution is N96L85 in the atmosphere, with 1.875° in longitude by 1.25° in latitude, 85 terrain-following hybrid height layers, and a model top at 85 km.

We use the atmosphere-only configuration of UKESM1 with prescribed present-day and future sea surface temperatures (SST) and sea ice (SICE) in the form of monthly mean time-evolving fields to investigate the transient impacts of changing emissions under different climates. These fields alongside global values for greenhouse gas and methane concentrations are generated from fully coupled UKESM1 runs for historical and future simulations conducted as part of the Coupled-Model

90 Intercomparison Project 6 (Eyring et al., 2016). We nudge the model with ERA-Interim meteorological reanalysis data for the present-day simulations, and allow the model to run freely in the simulations of future scenarios.

2.2 Emissions and experiments

We use CMIP6 year-2014 emissions, the latest year available, to represent present-day anthropogenic (Hoesly et al., 2018) and biomass burning emissions (Van Marle et al., 2017) for the globe, but replace anthropogenic emissions in China with
95 an up-to-date regional emission inventory over 2013-2017, the Multi-resolution Emission Inventory for China (MEIC; Li et al., 2017). Biogenic VOC emissions are calculated interactively with the iBVOC emissions scheme in the Joint UK Land Environmental Simulator (JULES) land-surface scheme (Pacifico et al., 2011), which is coupled to UKCA. Other online natural emissions such as sea salt, dust and lightning NO_x are the same as in UKESM1 simulations for CMIP6 (Turnock et al., 2020). Anthropogenic emissions for five sectors (industry, power plants, transport, residences, and agriculture) are provided for the
100 model, and independent diurnal and vertical emission profiles are applied for each sector (Bieser et al., 2011; Mailler et al., 2013).

For the future, emissions under the shared socio-economic pathways (SSPs) of CMIP6 are used that account for future social, economic, and environmental developments (O'Neill et al., 2014; Van Vuuren et al., 2014). We use the SSP1-1.9 pathway to represent Net Zero emission as net emissions of greenhouse gases drop down to zero at about 2060 in this scenario. We note
105 that this scenario has the potential to limit global warming to 1.5 degrees Celsius by the end of this century. Future scenarios for China are taken from the Dynamic Projection model for Emissions in China (DPEC; Tong et al., 2020), and we use the mbitious pollution neutral goal?scenario to represent a net zero pathway in China. For comparison, we use the SSP3-7.0 pathway from CMIP6, along with the corresponding aseline?scenario from DPEC, to represent a low mitigation scenario and to evaluate future O_3 pollution with high emissions. In addition, to assess the impacts of CH_4 on surface O_3, CH_4 concentrations from
110 SSP1-1.9 and SSP3-7.0 are used to represent low and high CH_4 respectively.

We perform several model experiments to investigate surface O_3 changes and to quantify the contribution of emission changes inside and outside China, global CH_4 concentrations, changes in climate, see Table 1. For each of the future scenarios the model is spun up for six years and then run for five years for data analysis. Table 2 summarises the global mean total surface emissions calculated from CMIP6, MEIC, and DPEC and the global CH_4 abundance.

115 2.3 Development of the deep learning model

A deep learning model is developed here to correct the biases in surface O_3 simulated with UKESM1. Like many other chemistry-climate models, UKESM1 exhibits systematic biases in surface O_3 (Turnock et al., 2020; Liu et al., 2022c; Archibald et al., 2020a), but it is hard to determine the origin of these biases. While some of these biases may be attributed to simplified chemistry, improvement in the chemical scheme in UKESM1 has been shown to increase biases in some locations (Archer-
120 Nicholls et al., 2021). However, this problem can be addressed through deep learning to simulate the differences between the chemistry-climate model simulations and real-world observations. The model is trained on present-day conditions to establish a relationship between O_3 biases and key outputs of the chemistry-climate model, referred to as features. Future O_3 biases

Table 1. Model configurations used for the present-day (2013-2017) and six future (2060-2070) simulations. ist.?means that the emissions, CH_4 concentrations or SST/SICE evolve as for the historical simulations. Z?means that they evolve under a net zero pathway. igh?means that they evolve under a high emission scenario, SSP3-7.0.

Experiment	Emis. in China	Emis. outside China	CH_4	SST/SICE
Present day	Hist.	Hist.	Hist.	Hist.
Net Zero	NZ	NZ	NZ	NZ
Local emis.	High	NZ	NZ	NZ
External emis.	NZ	High	NZ	NZ
High CH_4	NZ	NZ	High	NZ
Warmer climate	NZ	NZ	NZ	High
SSP3-7.0	High	High	High	High

Table 2. Overview of annual mean time-varying surface emissions of NO_x, VOCs, CO from anthropogenic (ANT), biomass burning (BB), and biogenic (BIO) sources for the present day (2013?017) and the future (2060?070) Net Zero and SSP3-7.0 pathway in China. Annual mean surface CH_4 mixing ratios (ppb) are also shown.

Emission (Tg(species)/yr)		Present day	Net Zero	SSP3-7.0
NO_x	ANT	24.2	2.9	33.9
	BB	0.3	0.2	0.3
	Total	24.5	3.1	34.2
VOCs	ANT	28.5	10.7	29.2
	BB	2.0	1.1	1.6
	BIO	38.0	56.4	56.9
	Total	68.5	68.2	87.6
CO	ANT	154.3	43.1	143.6
	BB	10.1	5.6	8.6
	Total	164.4	48.7	152.1
CH_4 (ppb)		1844.4	1266.6	2733.5

can then be predicted using features that are generated from simulations of the future with the chemistry-climate model. We adopt the approach applied by Liu et al. (2022b) to use 20 physical, meteorological and chemical variables as features , and these include variables associated with location, season, temperature, humidity, wind speed, photolysis and deposition rates

and concentrations of key precursors, see Liu et al. (2022b). We do not use O_3 concentration as a variable, as this is highly correlated with O_3 biases and thus masks the contribution of other factors. This approach has shown good performance in reproducing monthly mean surface O_3 biases over the globe, with a mean bias error of 0.1 ppb. In this study, we further develop and extend this deep learning model to predict the biases in daily mean O_3, which enables the examination of the occurrence of high O_3 episodes. We note that the CH_4 concentration is not included as an input feature because its variation under present-day conditions is much smaller than the changes expected in future. We therefore adopt the non-linear parameterisation developed by Wild et al. (2012) to quantify the response of surface O_3 to changing CH_4 concentrations in future, and consider this feature independently of the others.

The Chinese air quality reanalysis dataset (CAQRA; Kong et al., 2021) assimilates hourly mean surface O_3 observations during 2013-2017 from the China National Environmental Monitoring Centre (CNEMC), and we use this as a reference to derive surface O_3 biases in UKESM1 simulations. The surface O_3 reanalyses are shown to match observations well, with small mean errors of -2.3 g/m^3 (Kong et al., 2021). We account for these errors and uncertainties, and represent them as noise which we add to the original dataset in model training. We assume that this noise follows a normal distribution with a mean of 2.3 g/m^3 and one standard deviation of 2.3 g/m^3, and generate three datasets with random noise to reduce overfitting in training. The CAQRA data at 15 15 km resolution are regridded to the coarser resolution of UKESM1. A key advantage of the CAQRA data is that it provides complete spatial and temporal coverage for comparison with UKESM1, thus avoiding issues with the poor coverage of observations in some areas. However, we only examine data in areas below 2000 m altitude that have relatively high populations and where there are more measurement sites. For training, we pre-process the data to distribute them randomly across time and location, and then split them into a training set (80%), a validation set (10 %) and a testing set (10 %). The validation data are used to evaluate the model performance at each iteration of the training process, and the test data provide an independent evaluation when the model training is completed.

3 Future surface O_3 changes in China under Net Zero policies

Seasonal mean surface O_3 mixing ratios in China simulated with UKESM1 are shown in Fig. 1 for the present day and the Net Zero pathway, without bias correction. There is a clear seasonal variation in surface O_3, with high summertime O_3 and low wintertime O_3 (Fig. 1a, d). However, this variation is reduced under Net Zero (Fig. 1b, e) due to O_3 decreases in summer (Fig. 1c) and O_3 increases in parts of eastern China in winter (Fig. 1f) in future. Surface O_3 mixing ratios decrease by about 16 ppb in summer, demonstrating the great benefits of emission controls in mitigating summertime O_3 pollution. Other studies show similar results, with 18 ppb decreases in MDA8 O_3 mixing ratios achieved from Net Zero policies (Shi et al., 2021; Xu et al., 2022). However, smaller changes are seen in the most polluted industrial areas of China, namely the North China Plain, the Yangtze River Delta and the Pearl River Delta, even though reductions in anthropogenic emissions in these areas are substantially larger than other regions (Fig. S1a-b). This is principally due to VOC-limited O_3 formation regimes there in which decreased NO_x emissions increase O_3 mixing ratios (Liu et al., 2021). Much greater reductions in NO_x emissions or further reductions in VOC emissions are needed to reduce surface O_3 mixing ratios in these high-emission

regions. In contrast, higher emissions following SSP3-7.0 will greatly increase summertime O$_3$ (Fig. S2a-c), and the transport sector is shown to have the largest impact ~~on~~ with 10 ppb O$_3$ ~~changes~~increases.

In wintertime, ~~there are decreases in~~ surface O$_3$ mixing ratios ~~in less polluted areas but increases in heavily populated industrial regions, and increases of~~ generally decrease by 1 ppb in the mainland China, but increase in eastern China by up to 20 ppb ~~occur in eastern China~~in heavily populated industrial regions. This results in a reduced latitudinal gradient of O$_3$ mixing ratios in China in wintertime under the Net Zero scenario. These contrasting responses further demonstrate regional differences in the chemical environment for O$_3$ production. Polluted urban environments are dominated by VOC-limited O$_3$ formation, particularly in winter when weak boundary layer mixing permits greater NO$_x$ accumulation at the surface and rapid local O$_3$ destruction. Therefore, increased NO$_x$ emissions from the main emission sectors such as power plants, industry and transport under SSP3-7.0 cause notable decreases in O$_3$ mixing ratios of up to 3 ppb in winter (Fig. S2e-g) although the effect of the residential sector is relatively small (Fig. S2h) as small changes in NO$_x$ emissions are accompanied by substantial changes in VOC emissions (Cheng et al., 2021).
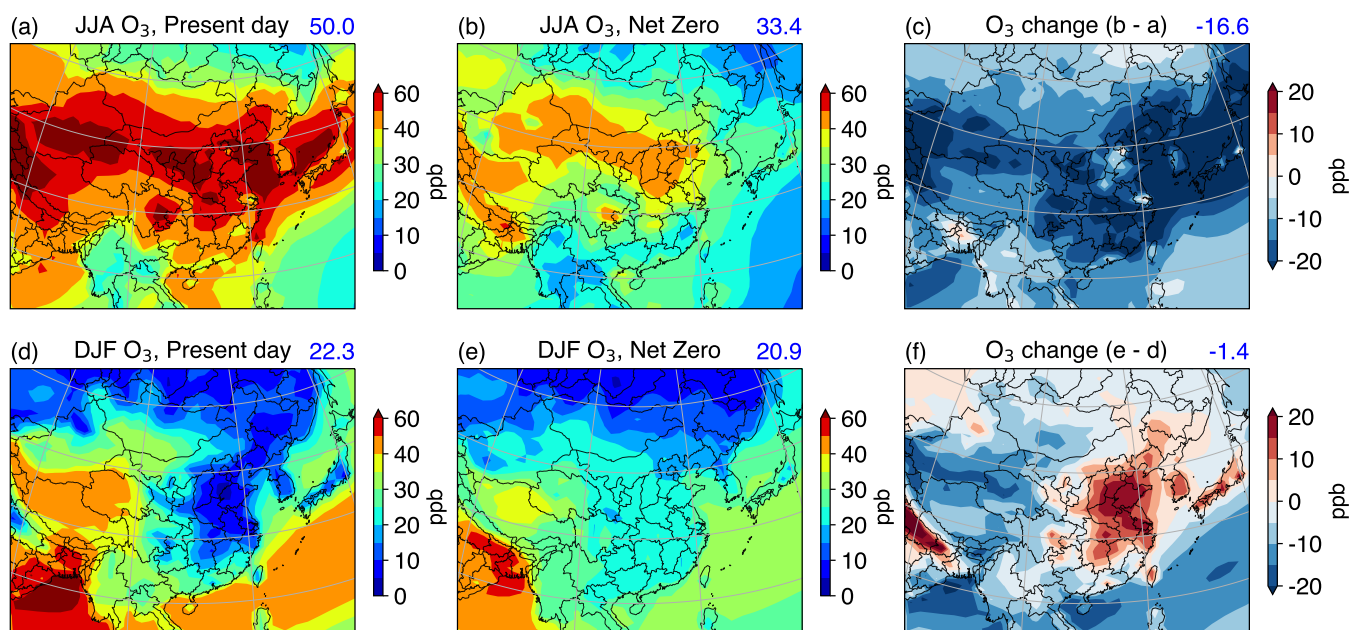
Figure 1. Seasonal surface O$_3$ mixing ratios in ~~China~~ East Asia simulated with UKESM1 from present day to the future following a Net Zero pathway. Mean O$_3$ mixing ratios are shown for June-July-August (JJA; **a, b**) and December-January-February (DJF; **d, e**) along with the corresponding seasonal changes (**c, f**), with values of O$_3$ changes in mainland China shown in ppb in the top right corner.

4 Drivers of future surface O$_3$ changes in China

While local emission changes directly influence surface O$_3$ changes in future, there are a number of other important drivers that govern surface O$_3$. We investigate four independent drivers: changes in emissions inside (Local emis.) and outside China (External emis.), changes in atmospheric CH$_4$ concentrations (High CH$_4$) and a warmer climate (Warmer climate) relative to the Net Zero pathway, see Fig. 2. Local anthropogenic emission changes in China are shown to have the largest impact in both seasons (Fig. 2a, e), but other drivers also contribute to surface O$_3$ changes and show substantial regional and seasonal differences.

The effect of changes in emissions outside China reflects the importance of transport of O$_3$ from other countries and higher background O$_3$ concentrations. If the rest of the world did not follow a Net Zero emission pathway, surface O$_3$ mixing ratios would be more than 10 ppb higher in summer (Fig. 2b). The contribution to O$_3$ in winter is generally smaller, estimated here as 4 ppb (Fig. 2f). The contribution of external emissions is much larger near the country borders than on central China. Changes in atmospheric CH$_4$ abundance have a relatively uniform influence on surface O$_3$ in eastern China, ~~and lead to O$_3$ increases of~~ with slightly greater effects in western China where altitudes are higher. A 4 ppb ~~in~~ O$_3$ increase due to higher CH$_4$ is seen for both seasons (Fig. 2c, g). The O$_3$ changes due to CH$_4$ are comparable to those across central China due to higher emissions outside China. In contrast, a warmer climate under the SSP3-7.0 scenario compared to the Net Zero pathway has minor impacts on surface O$_3$ changes (< 1 ppb). In general, surface O$_3$ mixing ratios decrease likely due to increased humidity under a warm climate but may increase locally due to higher temperatures, natural emissions and reduced O$_3$ deposition rates (Zanis et al., 2022). There are increased natural BVOC emissions in China under both Net Zero and SSP3-7.0 scenarios (Fig. S1c, f), particularly in southern China where vegetation is more abundant than in the north. Regional surface O$_3$ responds differently to different future climates (Fig. 2d, h), with O$_3$ increases in the south and O$_3$ decreases in the north under a warmer climate. The regional differences are consistent with those found under the effects of changing BVOC emissions in future (Liu et al., 2022a). These O$_3$ increases occur in both seasons but are more pronounced in summer. Overall, we show that while local emissions are critical to O$_3$ pollution, emissions outside China and global CH$_4$ concentrations are also important drivers of concern.

The seasonality of surface O$_3$ changes in China and globally are shown in Fig 3. In summer, local emissions dominate surface O$_3$ increases, while in winter and spring, O$_3$ transport from other countries and O$_3$ increases due to elevated CH$_4$ concentrations are more important. Strong NO titration of O$_3$ leads to substantial O$_3$ decreases in winter, but its effects are suppressed by more efficient O$_3$ production over summer (Fig. 3a). Emissions outside China increase O$_3$ mixing ratios throughout the year, with the greatest impact in late spring and early summer when intercontinental transport is strongest. The seasonal variation in the influence of local and external emissions is relatively small on a global scale, reflecting a limited sensitivity of global O$_3$ changes to emissions (Fig. 3b). The uniform influence of changes in CH$_4$ concentration is comparable both in China and globally. The warmer climate under SSP3-7.0 leads to slightly larger O$_3$ decreases on a global scale relative to the Net Zero scenario. We emphasize that seasonal O$_3$ responses to emission changes are more pronounced at a regional scale, and become weaker in winter, and that O$_3$ continental transport and background O$_3$ concentrations may still contribute to O$_3$ pollution.
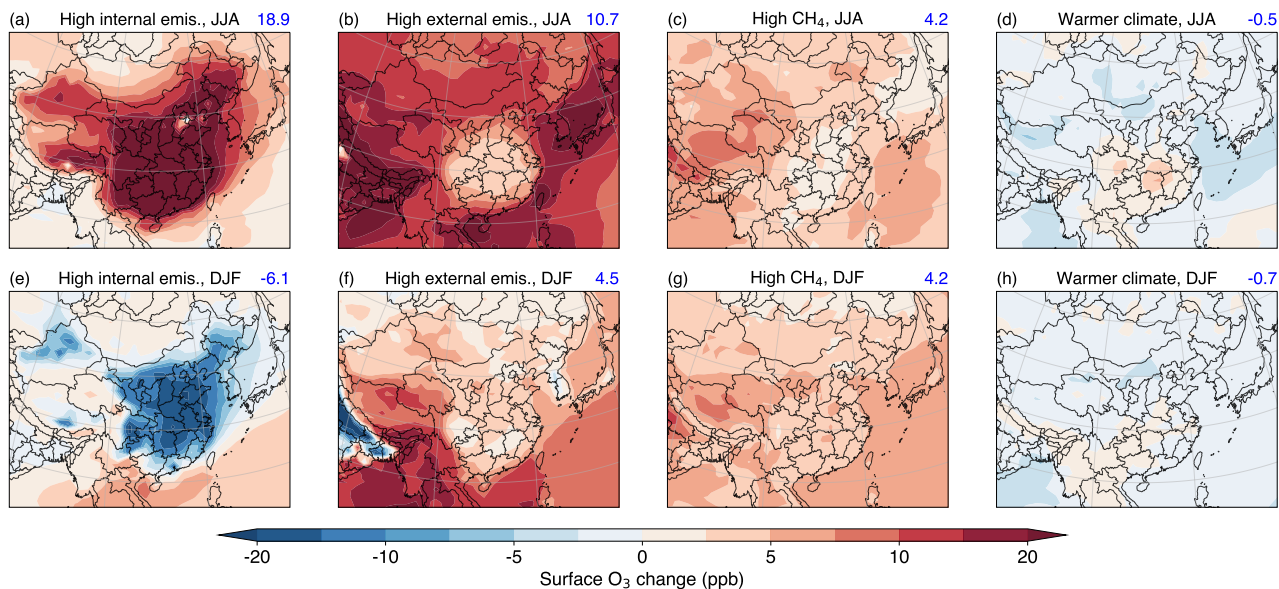
Figure 2. Contribution of changes in **(a)** internal emissions in ~~China~~East Asia, **(b)** external emissions outside China, **(c)** global CH_4 concentrations and **(d)** a warmer climate following the SSP3-7.0 pathway to seasonal surface O_3 changes relative to the Net Zero pathway. Mean O_3 changes over mainland China in ppb are shown in the top right corner.
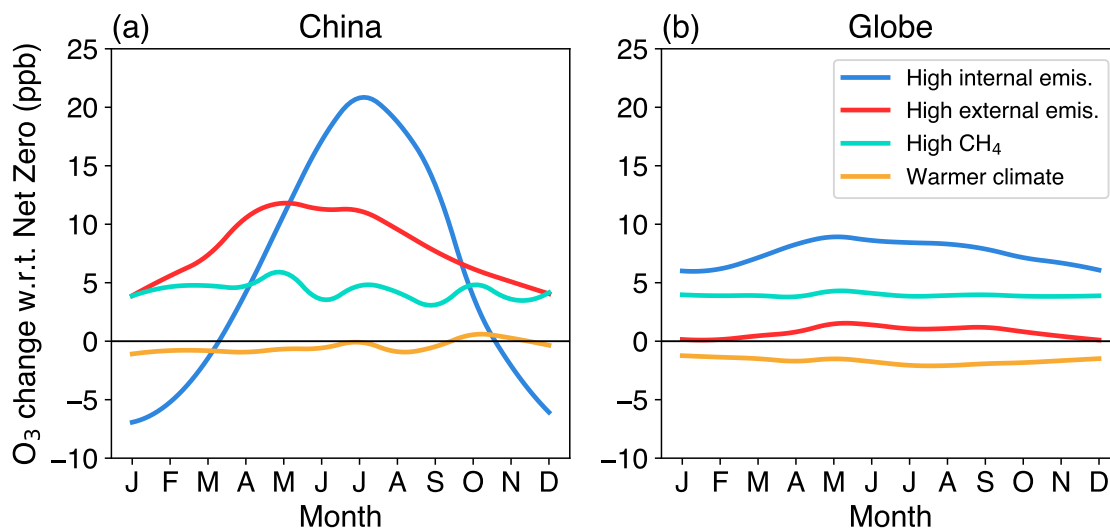
Figure 3. Seasonal surface O_3 changes relative to Net Zero due to changes in emissions in and outside China, global CH_4 concentrations and ~~a warmer~~ differences in 2060 climate under SSP3-7.0 in **(a)** China and **(b)** the globe.

205   To examine how the occurrence of high O_3 episodes may change in future, we show the frequency distributions of daily mean surface O_3 mixing ratios for all grid cells over China under different scenarios in Fig. 4. We find that surface O_3 mixing ratios under the Net Zero pathway follow an approximate normal distribution, with a mean O_3 of about 20 ppb (Fig. 4a). The frequency of high O_3 greater than 40 ppb can be greatly reduced under Net Zero. This is substantially different from the present day and SSP3-7.0 scenarios. SSP3-7.0 assumes that there are no emission controls in China, leading to a higher frequency of

210 high O_3 mixing ratios (> 50 ppb). However, the faster NO titration on O_3 with higher NO_x emissions also increases the frequency of low O_3 mixing ratios (< 10 ppb). In Fig. 4b, we show that the O_3 distribution shifts to higher values of O_3 under the high internal emission scenario and is substantially different from the other scenarios shown here, indicating that there is a large change in local O_3 production due to local emission changes. The frequency of O_3 mixing ratios between 30 and 50 ppb are highest in the scenarios of high external emissions and high CH_4 concentrations, demonstrating that these factors can lead

215 to an overall increase in daily mean O_3. In addition, we do not find significant changes in O_3 mixing ratios due to a warmer climate under SSP3-7.0.
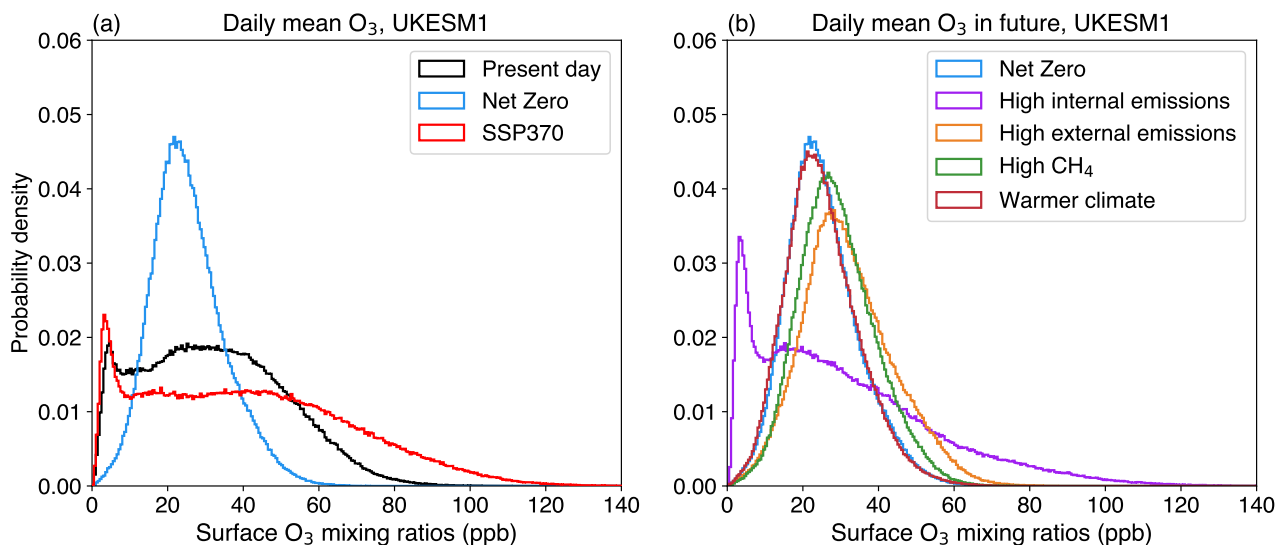
Figure 4. Whole year distributions of daily mean surface O_3 mixing ratios **(a)** in the present day, the Net Zero and the SSP3-7.0 scenarios in China, and **(b)** in the scenarios with higher internal emissions, external emissions, CH_4 concentrations and a warmer climate relative to Net Zero.

5   Bias corrected surface O_3 under the Net Zero pathway

Since there are systematic biases in surface O_3 simulations with UKESM1 (Fig. S3a, b), the reliability of future O_3 projections remains uncertain. We estimate the biases in surface O_3 through the deep learning model, and apply this to generate a more

220 robust assessment of O_3 changes under the Net Zero pathway. A fully independent evaluation for the deep learning model

is conducted using a testing dataset, see Fig. 5. We show that the magnitudes and distributions of biases in the UKESM1 simulations are reproduced well by the deep learning model, with a correlation coefficient of 0.96, a mean bias error of 0.1pb and a root-mean-square error of 4.0pb, which demonstrates the robustness of this approach. We also subtract the biases from UKESM1 and examine the spatial and temporal distribution of O_3 mixing ratios in China in Fig. 6. Spatial distributions of
225 surface O_3 in China over 2013-2017 can be also captured well (Fig. 6a, b, d, e), with the highest summertime O_3 and the lowest wintertime O_3 in the North China Plain. The magnitudes of surface O_3 mixing ratios with bias correction are in close agreement to the observations. The time series of daily mean O_3 can be also simulated well in Beijing and Guangzhou (Fig. 6c, f), which represent two different locations in northern and southern China with rather different chemical and meteorological environments. The evaluation demonstrates the capability of the deep learning model in correcting the seasonal and daily
230 UKESM1 simulation of surface O_3. This approach shows great promise in reducing current model errors, and hence has the potential to improve simulations of surface O_3 under future scenarios.
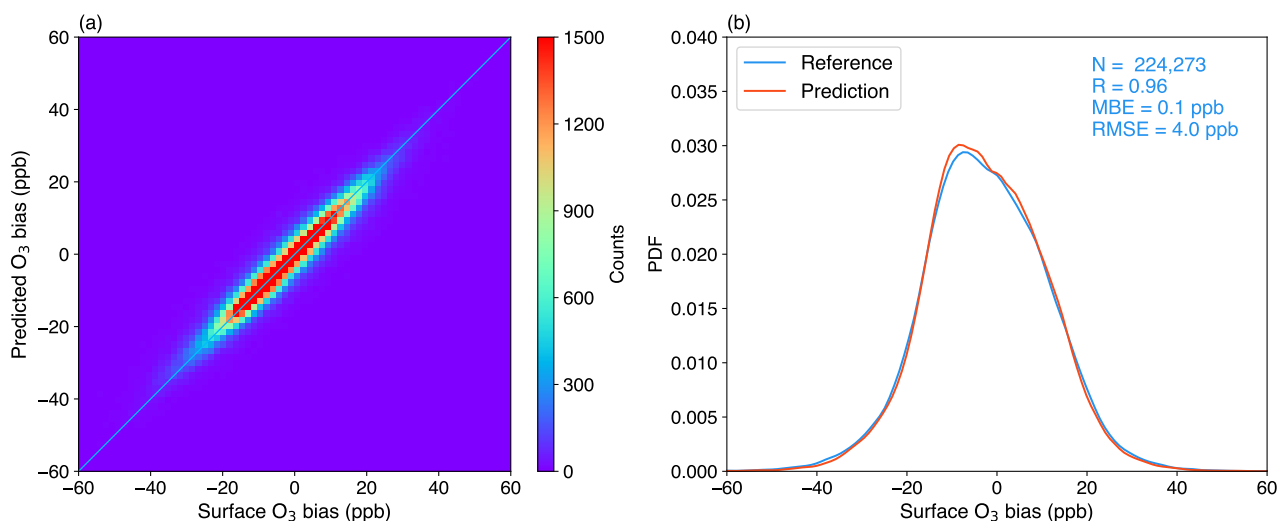
Figure 5. Independent evaluation of the deep learning model in simulating daily mean surface O_3 biases at each UKESM1 grid point over China. **(a)** Surface O_3 biases (UKESM1 minus CAQRA) and biases predicted by the deep learning model. **(b)** Probability density function (PDF) of O_3 biases (labelled here as Reference) and predicted O_3 biases. Statistics are shown in the top right corner.

Spatial distributions of future bias-corrected surface O_3 under the Net Zero pathway are shown in Fig. 7 to compare and contrast with UKESM1 outputs (Fig. 1), and to assess the effectiveness of emission controls. With bias correction, summertime O_3 mixing ratios generally decrease under Net Zero (Fig. 7a, b), consistent with UKESM1 results (Fig. 1c). We find that there
235 are larger O_3 decreases in summer in the North China Plain and the Yangtze River Delta (Fig. 7c) than in other less-polluted regions. However, the overall magnitudes of surface O_3 decreases are not as large as simulated with UKESM1. There are noticeable differences in the latitudinal mean surface O_3 decreases, with the maximum changes estimated as 10 ppb in the bias corrected simulation, smaller than 20 ppb predicted with UKESM1 (Fig. 7d). This indicates that the underlying impacts of
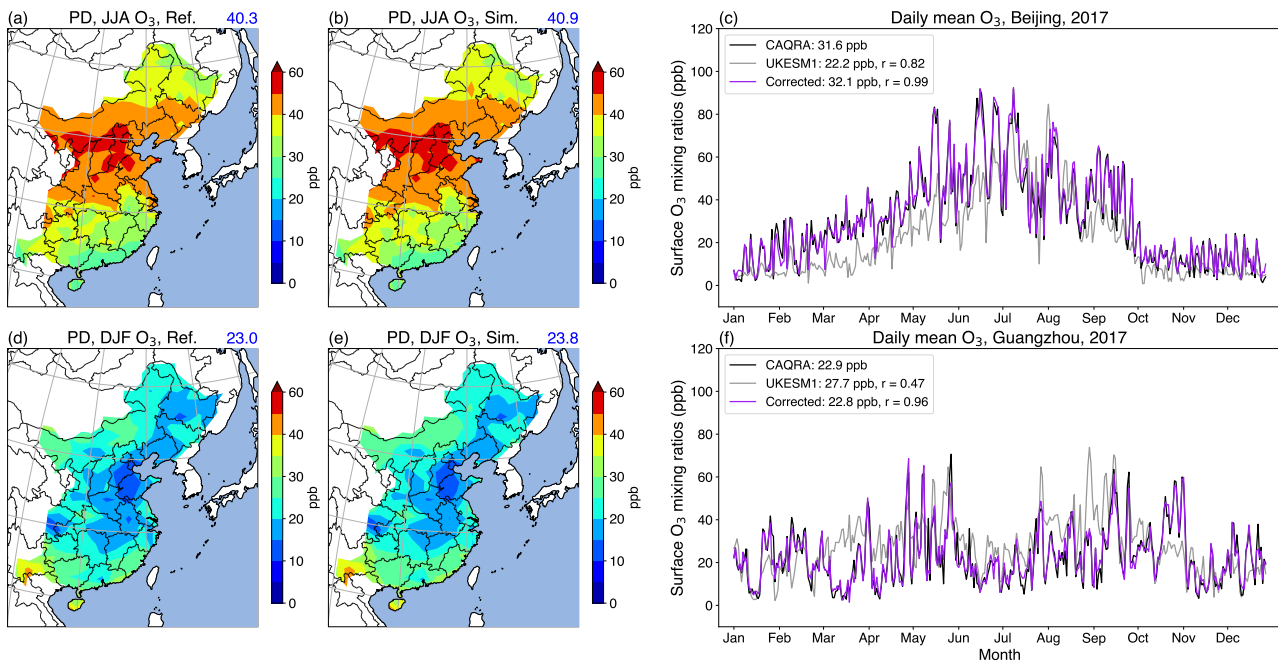
Figure 6. Surface mean O_3 mixing ratios derived from CAQRA (Ref.) in December-January-February (DJF) and June-July-August (JJA) over 2013-2017 **(a, d)**, compared with bias-corrected O_3 using deep learning **(b, e)**. Mean surface O_3 mixing ratios (ppb) over the Eastern part of mainland China are shown in the top right corner. Timeseries of daily mean O_3 mixing ratios in Beijing and Guangzhou in 2017 are shown in **(c, f)**, with mean O_3 values and correlation coefficients between CAQRA and the UKESM1 simulations and deep learning results shown in the legend.

emission controls on O_3 may not be as large as the model suggests, and that the O_3 responses to changing emissions may be
240   overestimated. This is also reflected in the overestimation of O_3 changes in southern China in the SSP3-7.0 scenario (Fig. S4a, b, c).

     In wintertime, while surface O_3 mixing ratios increase in high-emission regions under Net Zero, as seen in both UKESM1 and the bias-corrected results, areas with O_3 increases are smaller than those predicted by UKESM1 (Fig. 7). This again suggests that the magnitude and spatial extent of O_3 titration by NO may be overestimated in UKESM1. The same effect is
245   seen in the bias-corrected wintertime O_3 under SSP3-7.0 (Fig. S4). In general, biases in O_3 simulations from UKESM1 are smaller in the Net Zero scenario but still remain large in the SSP3-7.0 scenario (Fig. S3b-d). These two scenarios correspond to low and high emission pathways, respectively, which indicates that the accuracy of O_3 simulations in UKESM1 may decrease when emission changes become larger. The bias-corrected results show that only industrial regions with high NO_x emissions in China show substantial O_3 increases under Net Zero, while surface O_3 mixing ratios decrease in less polluted regions in
250   winter. This leads to a general decrease in latitudinal surface O_3 mixing ratios in wintertime (Fig. 7h).

With bias correction, the average surface O_3 mixing ratios are estimated to decrease in both seasons in the eastern part of China in the future under the Net Zero pathway. O_3 decreases of 5 ppb are predicted to occur in summer, which are slightly larger than the 4 ppb decreases predicted in winter. This demonstrates the overall advantages of net zero policies in achieving a surface ozone air quality co-benefit. Furthermore, in high-emission regions, the directions of surface O_3 changes are different in summer and winter, as shown in both UKESM1 and the corrected UKESM1, indicating that VOC-limited O_3 formation still dominates there in winter.
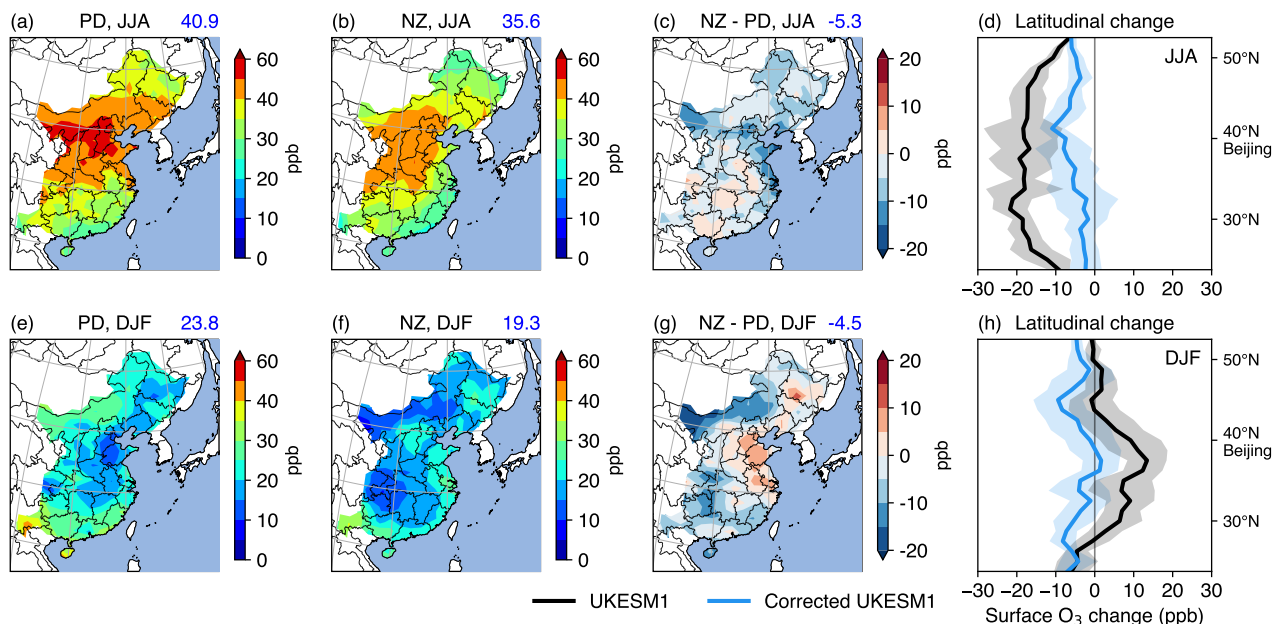
Figure 7. Seasonal mean surface O_3 mixing ratios corrected with the deep learning model in the present day (**a, b**) and the Net Zero scenario (**e, f**) in the Eastern part of mainland China, and the expected O_3 changes in summertime and wintertime (**c, g**). Latitudinal mean O_3 changes in UKESM1 and bias-corrected UKESM1 are shown in (**d, h**), where shading indicates one standard deviation of the changes in latitudinal O_3 mixing ratios.

We also calculate the annual average number of days with daily mean O_3 over 50 ppb as a measure to quantify high O_3 pollution episodes, see Fig. 8. The number of days per year with high O_3 episodes under present-day conditions can be reproduced well following bias correction (Fig. 8a, b, Table 3), with intensive areas of high O_3 pollution in the North China Plain (60 days) particularly in summertime, and relatively low occurrence in the Pearl River Delta (31 days). There is an average of 33 days per year with high O_3 pollution over China. We find that the Net Zero policies will succeed in reducing the number of high O_3 pollution days markedly by 65 % in future. In contrast, following higher emission control policies will increase high O_3 episodes by almost a factor of four (Table 3).

Following Net Zero emission controls, the Yangtze River Delta and the Pearl River Delta only have high O_3 episodes for a few days each year. However, high O_3 episodes still occur for almost one month (30 days) on the North China Plain and parts

of central China in the future, demonstrating that O$_3$ pollution cannot be fully eliminated in this region. The Sichuan basin is also a region where high O$_3$ pollution cannot be fully addressed, likely due to the favorable meteorological conditions leading to O$_3$ formation associated with the complex topography. Nevertheless, Net Zero policies are expected to deliver great benefits in mitigating O$_3$ pollution in China. Indeed, O$_3$ pollution is likely to become much worse if emissions continue to rise (Fig.
270   8d; Table 3). Even stricter controls on anthropogenic emissions than proposed to meet Net Zero may be required to avoid high O$_3$ pollution in the North China Plain.
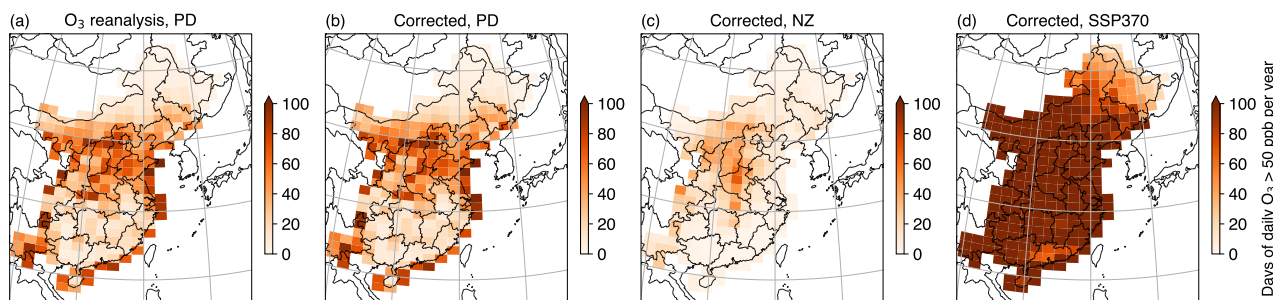
Figure 8. Annual average number of days with daily mean surface O$_3$ mixing ratios higher than 50 ppb in the present day calculated from **(a)** the surface O$_3$ reanalysis and **(b)** bias corrected UKESM1. Future high O$_3$ episodes under Net Zero **(c)** and SSP3-7.0 **(d)** pathways are shown from bias corrected UKESM1.

Table 3. Annual average number of days with daily mean surface O$_3$ mixing ratios higher than 50 ppb in China, the North China Plain (NCP), the Yangtze River Delta (YRD), the Pearl River Delta (PRD) and the Sichuan Basin (SCB). Conditions in the present day and under the Net Zero and SSP3-7.0 pathways are presented, calculated from the bias corrected UKESM1 simulations. The percentage change in the number of days in the future relative to the present day are shown.

Number of days with daily mean O$_3$ > 50 ppb/Regions	Present day (Reanalysis)	Present day (Corrected UKESM1)	Net Zero (Corrected UKESM1)	SSP3-7.0 (Corrected UKESM1)
China	32.1	33.9	11.9 (-65 %)	115.8 (242 %)
NCP	56.9	60.5	30.6 (-49 %)	123.7 (104 %)
YRD	45.0	45.3	4.8 (-89 %)	140.4 (210 %)
PRD	31.2	31.4	1.6 (-95 %)	117.0 (273 %)
SCB	34.4	34.1	16.5 (-52%)	139.3 (309 %)

6 Conclusions

Net Zero emission polices are important for reducing regional surface O_3 pollution as well as for mitigating climate change. We use a chemistry-climate model to quantify the O_3 changes in China under a Net Zero pathway, and investigate the relative importance of different drivers of these changes. We also place our results in context by comparing to a scenario, SSP3-7.0 in which weak climate mitigation leads to continued increases in precursor emissions. Surface O_3 responses to Net Zero emission control policies in China are distinctly different in different seasons, with substantial O_3 decreases in summer and O_3 increases in winter in high-emission regions due to decreased O_3 titration by NO. This demonstrates the large benefits of emission controls in reducing summertime average O_3 pollution in China by as much as 16 ppb.

Local emission changes are shown to be the most important driver influencing regional O_3 changes, which generally outweighs other drivers such as transport of O_3 from other countries, increased background O_3 formation through rising CH_4 abundance and a warmer climate. We do not find substantial changes in surface O_3 in China between Net Zero and SSP3-7.0 scenarios due to a warmer climate, but there are surface O_3 increases in southern China. Impacts of future local and external emissions on surface O_3 show strong seasonal variation, while increasing future CH_4 concentrations have a relatively uniform effect on O_3 throughout the year. In winter and spring, future external emissions outside China and higher CH_4 concentrations are more important than local emissions at a regional average scale.

We further demonstrate the capability of deep learning approaches to correct the biases in simulated daily mean O_3. UKESM1 shows systematic biases in simulated O_3 like many other chemistry-climate models; these are expected to influence their projections of future O_3. Deep learning can provide improved assessment of the impacts of Net Zero policies on surface O_3. We find that surface O_3 changes are overestimated by UKESM1 in summertime, and therefore the benefits of emission controls may be overestimated by chemistry-climate models. UKESM1 estimates that the mean latitudinal surface O_3 decreases due to emission controls could be up to 20 ppb in summer but bias correction shows that these may only be up to 10 ppb.

We acknowledge that there are uncertainties associated with the choice of deep learning model used and with the variables and parameters it is trained on, but the biases are sufficiently well predicted here that we are confident in the robustness of our results. The prediction might be further improved by employing more advanced deep learning architectures and considering a wider range of variables. The prediction of future surface O_3 biases may be slightly different under these conditions, but we believe that our principal results are likely to remain robust. The driving variables under the Net Zero scenario typically lie in the ranges associated with the present-day conditions that were used to train the model, suggesting that the relationships between inputs and outputs derived from the deep learning model are suitable for predicting future situations.

However, Net Zero emission policies succeed in reducing the number of days of high O_3 pollution by 65 % in China per year, with the number dropping from 33 days under present-day conditions to 11 days each year under Net Zero. The North China Plain will still be affected by high O_3 pollution in the future, meaning that stricter emission policies are needed in this region. In the Yangtze River Delta and the Pearl River Delta, O_3 pollution is likely to be less of a concern in the future as there are only a few days with high O_3 pollution under Net Zero. It is also clear that if emissions continue to rise, air quality in

China will be substantially worse than at present, and therefore emission controls are essential. However, it is clear from these studies that emission controls can be very effective in reducing surface O_3 pollution, and that Net Zero emission policies can substantially mitigate O_3 pollution in China.

Data availability. The data generated in this study are available upon request.

310 *Author contributions.* All authors participated in designing the study. ZL conducted UKESM1 simulations, built the deep learning model, and performed the analysis with input and discussions from OW, RD, FO'C and ST. ZL, OW and RD prepared the paper, with contributions from all co-authors.

Competing interests. The contact author has declared that none of the authors has any competing interests.

Acknowledgements. Zhenze Liu, Oliver Wild, Ruth M. Doherty thank the project of the UK-China collaboration to optimise net-zero policy
315 options for air quality and health (COP-AQ) under grants 2021GRIP02COP-AQ. Oliver Wild and Ruth M. Doherty thank the Natural Environment Research Council (NERC) for funding under grants NE/N006925/1, NE/N006976/1 and NE/N006941/1. Fiona M. O'Connor was supported by the Met Office Hadley Centre Climate Programme funded by BEIS and also acknowledges support from the EU Horizon 2020 Research Programme CRESCENDO (grant agreement number 641816). Steven Turnock would like to acknowledge support from the UKhina Research and Innovation Partnership Fund through the Met Office Climate Science for Service Partnership (CSSP) China as part of
320 the Newton Fund.

References

Archer-Nicholls, S., Abraham, N. L., Shin, Y., Weber, J., Russo, M. R., Lowe, D., Utembe, S., O'Connor, F., Kerridge, B., Latter, B., et al.: The Common Representative Intermediates Mechanism version 2 in the United Kingdom Chemistry and Aerosols Model, Journal of Advances in Modeling Earth Systems, 13, e2020MS002 420, 2021.

325 Archibald, A., Neu, J., Elshorbany, Y., Cooper, O., Young, P., Akiyoshi, H., Cox, R., Coyle, M., Derwent, R., Deushi, M., et al.: Tropospheric Ozone Assessment ReportA critical review of changes in the tropospheric ozone burden and budget from 1850 to 2100, Elementa: Science of the Anthropocene, 8, 2020a.

Archibald, A. T., O'Connor, F. M., Abraham, N. L., Archer-Nicholls, S., Chipperfield, M. P., Dalvi, M., Folberth, G. A., Dennison, F., Dhomse, S. S., Griffiths, P. T., et al.: Description and evaluation of the UKCA stratosphere–troposphere chemistry scheme (StratTrop vn

330 1.0) implemented in UKESM1, Geoscientific Model Development, 13, 1223–1266, 2020b.

Bieser, J., Aulinger, A., Matthias, V., Quante, M., and Van Der Gon, H. D.: Vertical emission profiles for Europe based on plume rise calculations, Environmental Pollution, 159, 2935–2946, 2011.

Brown, F., Folberth, G. A., Sitch, S., Bauer, S., Bauters, M., Boeckx, P., Cheesman, A. W., Deushi, M., Dos Santos Vieira, I., Galy-Lacaux, C., et al.: The ozone–climate penalty over South America and Africa by 2100, Atmospheric Chemistry and Physics, 22, 12 331–12 352,

335 2022.

Cheng, J., Tong, D., Zhang, Q., Liu, Y., Lei, Y., Yan, G., Yan, L., Yu, S., Cui, R. Y., Clarke, L., et al.: Pathways of China's $PM_{2.5}$ air quality 2015–2060 in the context of carbon neutrality, National Science Review, 8, nwab078, 2021.

Doherty, R., Wild, O., Shindell, D., Zeng, G., MacKenzie, I., Collins, W., Fiore, A. M., Stevenson, D., Dentener, F., Schultz, M., et al.: Impacts of climate change on surface ozone and intercontinental ozone pollution: A multi-model study, Journal of Geophysical Research:

340 Atmospheres, 118, 3744–3763, 2013.

Doherty, R. M.: Ozone pollution from near and far, Nature Geoscience, 8, 664–665, 2015.

Eyring, V., Bony, S., Meehl, G. A., Senior, C. A., Stevens, B., Stouffer, R. J., and Taylor, K. E.: Overview of the Coupled Model Intercomparison Project Phase 6 (CMIP6) experimental design and organization, Geoscientific Model Development, 9, 1937–1958, 2016.

Fiore, A. M., Naik, V., and Leibensperger, E. M.: Air quality and climate connections, Journal of the Air & Waste Management Association,

345 65, 645–685, 2015.

Griffiths, P. T., Murray, L. T., Zeng, G., Shin, Y. M., Abraham, N. L., Archibald, A. T., Deushi, M., Emmons, L. K., Galbally, I. E., Hassler, B., et al.: Tropospheric ozone in CMIP6 simulations, Atmospheric Chemistry and Physics, 21, 4187–4218, 2021.

Hedegaard, G. B., Christensen, J. H., and Brandt, J.: The relative importance of impacts from climate change vs. emissions change on air pollution levels in the 21st century, Atmospheric Chemistry and Physics, 13, 3569–3585, 2013.

350 Hoesly, R. M., Smith, S. J., Feng, L., Klimont, Z., Janssens-Maenhout, G., Pitkanen, T., Seibert, J. J., Vu, L., Andres, R. J., Bolt, R. M., et al.: Historical (1750–2014) anthropogenic emissions of reactive gases and aerosols from the Community Emissions Data System (CEDS), Geoscientific Model Development, 11, 369–408, 2018.

Hollaway, M., Wild, O., Yang, T., Sun, Y., Xu, W., Xie, C., Whalley, L., Slater, E., Heard, D., and Liu, D.: Photochemical impacts of haze pollution in an urban environment, Atmospheric Chemistry and Physics, 19, 9699–9714, 2019.

355 Hong, C., Zhang, Q., Zhang, Y., Davis, S. J., Tong, D., Zheng, Y., Liu, Z., Guan, D., He, K., and Schellnhuber, H. J.: Impacts of climate change on future air quality and human health in China, Proceedings of the national academy of sciences, 116, 17 193–17 200, 2019.

Hornik, K., Stinchcombe, M., and White, H.: Multilayer feedforward networks are universal approximators, Neural networks, 2, 359–366, 1989.

IPCC: Climate Change 2022: Mitigation of Climate Change. Contribution of Working Group III to the Sixth Assessment Report of the Intergovernmental Panel on Climate Change, IPCC, 2022.

Kong, L., Tang, X., Zhu, J., Wang, Z., Li, J., Wu, H., Wu, Q., Chen, H., Zhu, L., Wang, W., et al.: A 6-year-long (2013–2018) high-resolution air quality reanalysis dataset in China based on the assimilation of surface observations from CNEMC, Earth System Science Data, 13, 529–570, 2021.

LeCun, Y., Bengio, Y., and Hinton, G.: Deep learning, nature, 521, 436–444, 2015.

Li, K., Jacob, D. J., Shen, L., Lu, X., De Smedt, I., and Liao, H.: Increases in surface ozone pollution in China from 2013 to 2019: anthropogenic and meteorological influences, Atmospheric chemistry and physics, 20, 11 423–11 433, 2020.

Li, M., Liu, H., Geng, G., Hong, C., Liu, F., Song, Y., Tong, D., Zheng, B., Cui, H., Man, H., et al.: Anthropogenic emission inventories in China: a review, National Science Review, 4, 834–866, 2017.

Li, M., Zhang, Q., Zheng, B., Tong, D., Lei, Y., Liu, F., Hong, C., Kang, S., Yan, L., Zhang, Y., et al.: Persistent growth of anthropogenic non-methane volatile organic compound (NMVOC) emissions in China during 1990–2017: drivers, speciation and ozone formation potential, Atmospheric Chemistry and Physics, 19, 8897–8913, 2019.

Liu, S., Sahu, S. K., Zhang, S., Liu, S., Sun, Y., Liu, X., Xing, J., Zhao, B., Zhang, H., and Wang, S.: Impact of Climate-Driven Land-Use Change on O3 and PM Pollution by Driving BVOC Emissions in China in 2050, Atmosphere, 13, 1086–, 2022a.

Liu, Z., Doherty, R. M., Wild, O., Hollaway, M., and O'Connor, F. M.: Contrasting chemical environments in summertime for atmospheric ozone across major Chinese industrial regions: the effectiveness of emission control strategies, Atmospheric Chemistry and Physics, 21, 10 689–10 706, 2021.

Liu, Z., Doherty, R. M., Wild, O., O'Connor, F. M., and Turnock, S. T.: Correcting ozone biases in a global chemistry–climate model: implications for future ozone, Atmospheric Chemistry and Physics, 22, 12 543–12 557, 2022b.

Liu, Z., Doherty, R. M., Wild, O., O'connor, F. M., and Turnock, S. T.: Tropospheric ozone changes and ozone sensitivity from the present day to the future under shared socio-economic pathways, Atmospheric Chemistry and Physics, 22, 1209–1227, 2022c.

Mailler, S., Khvorostyanov, D., and Menut, L.: Impact of the vertical emission profiles on background gas-phase pollution simulated from the EMEP emissions over Europe, Atmospheric Chemistry and Physics, 13, 5987–5998, 2013.

Morgenstern, O., Braesicke, P., O'connor, F., Bushell, A., Johnson, C., Osprey, S., and Pyle, J.: Evaluation of the new UKCA climate-composition model–Part 1: The stratosphere, Geoscientific Model Development, 2, 43–57, 2009.

Mulcahy, J. P., Johnson, C., Jones, C. G., Povey, A. C., Scott, C. E., Sellar, A., Turnock, S. T., Woodhouse, M. T., Abraham, N. L., Andrews, M. B., et al.: Description and evaluation of aerosol in UKESM1 and HadGEM3-GC3. 1 CMIP6 historical simulations, Geoscientific Model Development, 13, 6383–6423, 2020.

O'Connor, F., Johnson, C., Morgenstern, O., Abraham, N., Braesicke, P., Dalvi, M., Folberth, G., Sanderson, M., Telford, P., Voulgarakis, A., et al.: Evaluation of the new UKCA climate-composition model–Part 2: The Troposphere, Geoscientific Model Development, 7, 41–91, 2014.

O'Neill, B. C., Kriegler, E., Riahi, K., Ebi, K. L., Hallegatte, S., Carter, T. R., Mathur, R., and Van Vuuren, D. P.: A new scenario framework for climate change research: the concept of shared socioeconomic pathways, Climatic change, 122, 387–400, 2014.

Pacifico, F., Harrison, S., Jones, C., Arneth, A., Sitch, S., Weedon, G., Barkley, M., Palmer, P., Serça, D., Potosnak, M., et al.: Evaluation of a photosynthesis-based biogenic isoprene emission scheme in JULES and simulation of isoprene emissions under present-day climate conditions, Atmospheric Chemistry and Physics, 11, 4371–4389, 2011.

Parrish, D. D., Derwent, R. G., Turnock, S. T., O'Connor, F. M., Staehelin, J., Bauer, S. E., Deushi, M., Oshima, N., Tsigaridis, K., Wu, T., et al.: Investigations on the anthropogenic reversal of the natural ozone gradient between northern and southern midlatitudes, Atmospheric Chemistry and Physics, 21, 9669–9679, 2021.

Revell, L. E., Stenke, A., Tummon, F., Feinberg, A., Rozanov, E., Peter, T., Abraham, N. L., Akiyoshi, H., Archibald, A. T., Butchart, N., et al.: Tropospheric ozone in CCMI models and Gaussian process emulation to understand biases in the SOCOLv3 chemistry–climate model, Atmospheric chemistry and physics, 18, 16 155–16 172, 2018.

Sellar, A. A., Jones, C. G., Mulcahy, J. P., Tang, Y., Yool, A., Wiltshire, A., O'connor, F. M., Stringer, M., Hill, R., Palmieri, J., et al.: UKESM1: Description and evaluation of the UK Earth System Model, Journal of Advances in Modeling Earth Systems, 11, 4513–4558, 2019.

Shi, X., Zheng, Y., Lei, Y., Xue, W., Yan, G., Liu, X., Cai, B., Tong, D., and Wang, J.: Air quality benefits of achieving carbon neutrality in China, The Science of the total environment, 795, 148 784–148 784, 2021.

Tay, A.: By the numbers: China's net-zero ambitions., Nature, 2022.

Tong, D., Cheng, J., Liu, Y., Yu, S., Yan, L., Hong, C., Qin, Y., Zhao, H., Zheng, Y., Geng, G., et al.: Dynamic projection of anthropogenic emissions in China: methodology and 2015–2050 emission pathways under a range of socio-economic, climate policy, and pollution control scenarios, Atmospheric Chemistry and Physics, 20, 5729–5757, 2020.

Turnock, S. T., Allen, R. J., Andrews, M., Bauer, S. E., Deushi, M., Emmons, L., Good, P., Horowitz, L., John, J. G., Michou, M., et al.: Historical and future changes in air pollutants from CMIP6 models, Atmospheric Chemistry and Physics, 20, 14 547–14 579, 2020.

UNEP: Emissions Gap Report 2022: The Closing Window — Climate crisis calls for rapid transformation of societies, 2022.

Van Marle, M. J., Kloster, S., Magi, B. I., Marlon, J. R., Daniau, A.-L., Field, R. D., Arneth, A., Forrest, M., Hantson, S., Kehrwald, N. M., et al.: Historic global biomass burning emissions for CMIP6 (BB4CMIP) based on merging satellite observations with proxies and fire models (1750–2015), Geoscientific Model Development, 10, 3329–3357, 2017.

Van Vuuren, D. P., Kriegler, E., O'Neill, B. C., Ebi, K. L., Riahi, K., Carter, T. R., Edmonds, J., Hallegatte, S., Kram, T., Mathur, R., et al.: A new scenario framework for climate change research: scenario matrix architecture, Climatic Change, 122, 373–386, 2014.

Walters, D., Baran, A. J., Boutle, I., Brooks, M., Earnshaw, P., Edwards, J., Furtado, K., Hill, P., Lock, A., Manners, J., et al.: The Met Office Unified Model global atmosphere 7.0/7.1 and JULES global land 7.0 configurations, Geoscientific Model Development, 12, 1909–1963, 2019.

Wang, T., Xue, L., Feng, Z., Dai, J., Zhang, Y., and Tan, Y.: Ground-level ozone pollution in China: a synthesis of recent findings on influencing factors and impacts, Environmental Research Letters, 17, 063 003, 2022a.

Wang, W., Parrish, D. D., Wang, S., Bao, F., Ni, R., Li, X., Yang, S., Wang, H., Cheng, Y., and Su, H.: Long-term trend of ozone pollution in China during 2014–2020: distinct seasonal and spatial characteristics and ozone sensitivity, Atmospheric chemistry and physics, 22, 8935–8949, 2022b.

WHO: Global air quality guidelines: particulate matter ($PM_{2.5}$ and PM_{10}), ozone, nitrogen dioxide, sulfur dioxide and carbon monoxide: executive summary, 2021.

Wild, O., Fiore, A. M., Shindell, D., Doherty, R., Collins, W., Dentener, F., Schultz, M., Gong, S., MacKenzie, I., Zeng, G., et al.: Modelling future changes in surface ozone: a parameterized approach, Atmospheric Chemistry and Physics, 12, 2037–2054, 2012.

Wild, O., Voulgarakis, A., O'Connor, F., Lamarque, J.-F., Ryan, E. M., and Lee, L.: Global sensitivity analysis of chemistry–climate model budgets of tropospheric ozone and OH: exploring model diversity, Atmospheric Chemistry and Physics, 20, 4047–4058, 2020.

Xu, B., Wang, T., Ma, D., Song, R., Zhang, M., Gao, L., Li, S., Zhuang, B., Li, M., and Xie, M.: Impacts of regional emission reduction and global climate change on air quality and temperature to attain carbon neutrality in China, Atmospheric research, 279, 106 384–, 2022.

435 Young, P. J., Naik, V., Fiore, A. M., Gaudel, A., Guo, J., Lin, M., Neu, J., Parrish, D., Rieder, H., Schnell, J., et al.: Tropospheric Ozone Assessment Report: Assessment of global-scale model performance for global and regional ozone distributions, variability, and trends, Elementa: Science of the Anthropocene, 6, 2018.

Zanis, P., Akritidis, D., Turnock, S., Naik, V., Szopa, S., Georgoulias, A. K., Bauer, S. E., Deushi, M., Horowitz, L. W., Keeble, J., et al.: Climate change penalty and benefit on surface ozone: a global perspective based on CMIP6 earth system models, Environmental Research

440 Letters, 17, 024 014, 2022.

Zeng, G., Pyle, J., and Young, P.: Impact of climate change on tropospheric ozone and its global budgets, Atmospheric Chemistry and Physics, 8, 369–387, 2008.

Zhang, Q., Zheng, Y., Tong, D., Shao, M., Wang, S., Zhang, Y., Xu, X., Wang, J., He, H., Liu, W., et al.: Drivers of improved PM2. 5 air quality in China from 2013 to 2017, Proceedings of the National Academy of Sciences, 116, 24 463–24 469, 2019.